Journal of Operation and Automation in Power Engineering
Vol. 8, No. 3, Dec. 2020, Pages: 234-244
http://joape.uma.ac.ir

Estimation of New Weighted Controlled Switching Overvoltage by RBFN Model

M. Hasanpour [1], M. Ghanbari [1], V. Parvin-Darabad [1, 2]*

[1]Department of Electrical Engineering, Gorgan Branch, Islamic Azad University, Gorgan, Iran
[2] Department of Electrical Engineering, Golestan University, Gorgan, Iran

Abstract- *Mitigating switching overvoltages (SOVs) and conducting well-suited insulation coordination for handling stresses are very important in UHV transmission Lines. The best strategy in the absence of arresters is controlled switching (CS). Although elaborate works on electromagnetic transients are considered in the process of designing transmission systems, such works are not prevalent in day-to-day operations. The power utility and/or operator have to carefully monitor the peak values of SOVs so this values not to exceed the safe limits. In this paper, we present a novel CS approach in dealing with EMTP/ATP environment, where trapped charge (TC) is intended to train a radial basis function network (RBFN) meta-model that is implemented to calculate SOVs. A new weighted maximum overvoltage factor proposed to find locations of critical failure risk due to SOVs occurred along transmission lines. Power utilities or design engineers can benefit from the presented meta-model in designing a well-suited insulation level without spending time for taking into account the feasible risk value. Besides, the operators can energize the lines sequentially upon their choice; i.e., a safe and proper energization.*

Keyword: Switching overvoltage, Transmission line, Controlled switching, RBFN.

1. INTRODUCTION

With regard to the undeniable role of electrical energy in modern societies, the problem of blackouts is very significant. Therefore, regional electricity companies and large-scale customers have been trying to prevent blackouts. A large part of the electrical energy is transmitted by the transmission lines, so the importance of transmission line protection for continuous power transmission is crucial [1]. The investigation, control and simulation of SOVs to achieve an appropriate insulation coordination in both design and operation stages require sophisticated knowledge of transmission line transients [2]. Moreover, as the power grid gradually develops, the study of SOVs encounters some complexities in the design stage. In the operation stage, it is challenging for the operator to determine the sequence of transmission lines energization in order to keep the SOV within the allowable limits. This challenge has been studied in various research works.

In some studies [3-9], artificial neural networks have been used as black boxes for equivalent nonlinear systems and to simplify the complexities of real systems. In Ref. [3], an artificial neural network is used to estimate the behavior of a medium voltage feeder against changes in temperature and humidity for the optimal load management. In Ref. [4], an intelligent network is used to estimate the distribution network harmonics and thereby to reduce the number of monitoring units as much as possible. A system for controlled switching (CS) of high voltage circuit breakers, which can determine the closing time of phases with regard to the trapped charge (TC), uncertainties of circuit breaker (CB) and the controller circuit, as well as the pre-strike voltage, has not been developed so far [5-9]. In Ref. [8], the most comprehensive study on the overvoltage of conventional CBs has been carried out. In this study, the insulation risk has been calculated using the structural specifications of the line and taking into account the height profile, TC and surge arrester installation. Then, the critical points of failure for each power grid are predicted using an intelligent network. This study only focuses on installing surge arresters to reduce the overvoltage, and similar to some previous studies [5-7], it does not account for the effective parameter of pre-strike voltage. In Ref. [9], in accordance with [8], the SOV of a 500 kV line has been estimated using a fuzzy-neural network.

Various studies have also been conducted on CS without considering the TC [10-12]. In the most

Received: 22 Feb. 2020
Revised: 03 May 2020
Accepted: 10 May 2020
∗Corresponding author:
E-mail: Ghanbari@gorganiau.ac.ir (M. Ghanbari)
Digital object identifier: 10.22098/joape.2020.6987.1508
Research Paper

prominent of these studies [10], CS has been roughly performed because the closing instant is determined by using the TC polarity. Subsequently, statistical switching has been implemented using the predetermined mean and standard deviation values. However, these values must be determined based on the circuit breaker characteristics. Reference [12] uses an ABB F236 controller to perform CS on a transmission line. This commercial controller is equipped with zero-crossing of the source side waveform for the transmission line energization. The performance of this controller is studied for the statistical switching of CS. However, this method cannot be used to include TC voltage in reclosing operations.

Recent studies [13-15] have introduced new CS methods during the reclosing of a transmission line after short circuit faults. However, these studies do not consider worst-case caused by the TC during reclosing. Reference [16] proposes a new method based on the combination of closing instant control and pre-insertion resistor in the presence or absence of compensating reactor. This study, similar to Ref. [10], investigates the CS using TC polarity although to increase its applicability, the presence of the reactor is considered. Moreover, while combining of closing control and pre-insertion resistor increases the reliability of the one-and-a-half-breaker scheme, the reduction in overvoltage is not significant enough and surge arresters are required.

The purpose of the present paper is to define a neural network to predict the location and magnitude of weighted SOVs during CS of CBs. Accordingly, this artificial network can be used by employing the structural specifications of the line and parameters of CBs for every transmission line. In this paper, sensitivity analyses are performed for all parameters affecting the maximum value of SOV.

Indeed, using an intelligent network trained in the operation stage, it is possible to determine the sequence of high voltage lines energization. Moreover, using this intelligent network in the design stage of a developed grid, the optimal value of the insulation strength of the lines can be determined at different points of the grid. Therefore, in the process of insulation design and operation, the trained network can be used instead of modeling the real power grid. The main contributions of this paper are as follows:

- Considering all parameters affecting the proposed CS strategy, including TC and pre-strike voltage.
- Absence of disturbances due to TC fluctuations.
- Presenting the simple and accurate criterion of weighted voltage for evaluating insulation coordination.
- Training the radial basis function network (RBFN) for predicting weighted voltages and using its simple and accurate calculations.
- Determining the critical points of the transmission line during line energization using CS.
- Ability to use the trained network during line energization in the operation stage.

2. WEIGHTED MAXIMUM OVERVOLTAGE

Due to the randomness of the parameters affecting the SOV amplitude, it is necessary to perform a statistical study to obtain the maximum overvoltage amplitude along the line. CS of circuit breakers is also no exception to this rule and experiences uncertainty; it is necessary to use switching statistics to investigate overvoltages due to the closing of circuit breakers. The statistical switching is performed through many switching operations, for example, 100 switching operations. The closing time determines uniform distribution around the mean value with a standard deviation [2]. The mean value (μ) and standard deviation (σ) are calculated by the case peak method so that in each switching operation, the highest peak value and phase-to-earth or phase-to-phase overvoltages are included in the voltage probability distribution. Each energization yields one data point and the highest peak as well as phase-to-earth and phase-to-phase overvoltages. The SOV peak values of all three phase and between phases are collected in a normal distribution function as follows:

$$p(x)=\frac{1}{\sigma\sqrt{2\pi}}e^{-\frac{1}{2}\left(\frac{x-\mu}{\sigma}\right)^2} \quad (1)$$

Where, μ and σ are, respectively, the mean and standard deviation of SOV respectively. Deviation and truncation values are, respectively, given by:

$$\sigma_e = 0.17(U-1) \quad (2)$$

$$U_e = 1.13U - 0.13 \quad (3)$$

Where, U denotes SOVs with 2% probability of being exceeded.

2.1. Maximum overvoltage

The 400 kV system under study is located in southern Iran. The analysis is performed on a line of the system according to the single-line diagram of Fig. 1 [7].

The label of the line implemented in the electromagnetic transient program/ alternative transient program (EMTP/ATP) software is SA913 as shown in Fig. 2. The feeding substation is modeled by an AC

supply. Thevenin equivalent impedance behind the source is implemented using the "LINE RL" block.

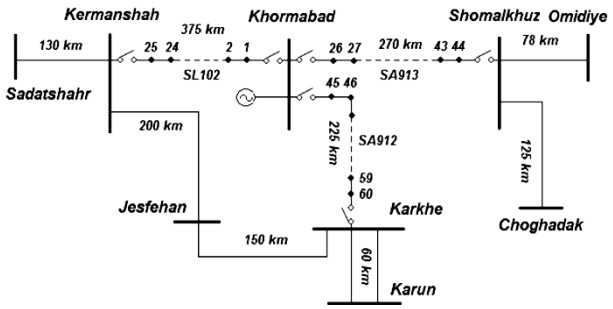

Fig. 1. Single line diagram of the case study

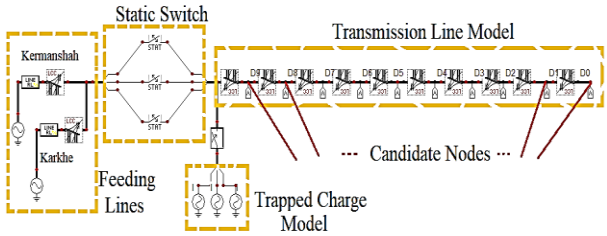

Fig. 2. ATPDraw implementation of the case study

The short-circuit impedances of substations are calculated using the short-circuit calculations, and the results are presented in Table 1. To implement the feeding network in switching studies, it is necessary to consider the receiving feeding lines up to the first receiving substation [13]. The receiving substations are Karkheh and Kermanshah substations that feed the line under study through lines SA912 and SL102. Therefore, in studying switching, the line SA913 up to the mentioned substations has to be implemented as shown in Fig. 2.

The statistical circuit breaker, "STAT", is another implemented part that makes the statistical switching process possible. The mean and standard deviation at the closing instant have to be determined for this CB. The transmission line SA913 is implemented using the "LCC" block, and finally, the default ATP current source for TC is used to model the TC in the line.

Table 1. Impedance behind the source of substations of the network under study [7]

Power station Name	R_0 (Ω)	X_0 (Ω)	R_+ (Ω)	X_+ (Ω)	Source Power (MVA)
Khoramabad	72	320	24.48	215.65	737.32
Kermanshah	30.4	88.65	2.88	32.96	1000.66
Shomal Khuzestan	8.69	32.32	0.96	15.04	2512.69
Karkhe	7.52	32.32	0.96	14.40	2578.68
Karun	0.96	11.2	0.48	8.16	5799.35
Choghadak	2.4	14.4	1.12	15.2	3549.16
Jesfehan	0.96	8.32	.480	7.68	6732.54
Omodiyeh	7.2	24.32	0.96	10.72	3412.30
Saadatshahr	52.16	157.6	0.96	15.04	815.71

Therefore, each transmission line is modeled using the three-bus system. The ATP software is used to determine the statistical distribution function of switching SOV [14]. Statistical switching is performed by changing the switching voltage angle, which is equivalent to changing the amplitude of the source at the closing instant. To obtain the probability distribution function of overvoltages, CBs must be closed at random times [19]. The probability distribution of closing instants includes mean and standard deviation values for each phase. The mean values are determined using the method proposed in this paper. Standard deviation depends on the errors of the mechanical system and the controller circuit. The CB in this study, which is used to feed a 400 kV, 50 Hz transmission line, has two arc extinguishing chambers, and its closing speed is 170 kilovolts per millisecond with a standard deviation of 0.35 milliseconds [20].

For obtaining the statistical distribution of the closing instants of each phase, similar to the case of a random process, it is necessary to perform statistical switching for a number of times, for example, 100 times. Therefore, the statistical switching tool of ATP software is used.

After performing 100 statistical switching operations, the ATP software calculates the maximum and minimum of generated voltages, taking account of their polarity, at the candidate points D_0 to D_9. Since the amplitude of a destructive overvoltage may cause an insulation failure, the largest overvoltage amplitude is extracted.

2.2. Weight function of overvoltage

In the process of transmission line insulation coordination, not only the generated overvoltage has a direct effect on insulation failure of insulator strings, but the insulation strength of each of the insulators is also determinative. In principle, at the design stage of the line, the insulation levels of all insulator strings in the line are assumed to be the same.

It is assumed that the probability of disruptive discharge of insulation is given by a normal cumulative probability function [21]:

$$P(V)=\frac{1}{\sigma\sqrt{2\pi}}\int_{-\infty}^{V} e^{-\frac{(V-CFO)^2}{2\sigma^2}}dV \qquad (4)$$

where P(V) is the probability of disruptive discharges, σ is the standard deviation and critical flashover voltage (CFO), i.e., the voltage under which the insulation has a 50% probability of flashover or withstand. The CFO is determined if the basic switching impulse insulation level (BSL) of the line is specified.

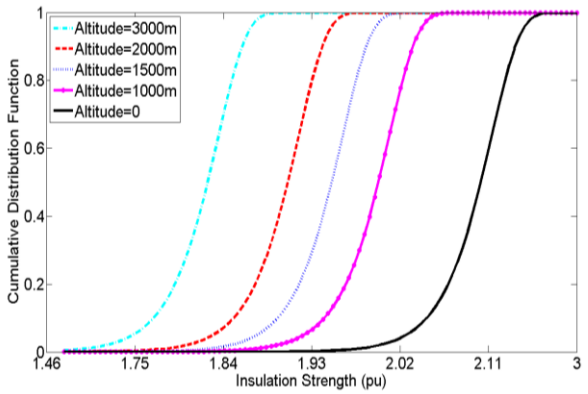

Fig. 3. Effect of increasing line height above sea level on insulation strength (CFO_n) of insulators (V_{base}=342928 volts)

$$BSL = CFO(1-1.28\frac{\sigma}{CFO}) \quad (5)$$

However, due to the changes in the height profile of the line towers above sea level, the insulators installed at higher altitudes are more vulnerable compared to those installed at a lower altitude. At different heights of towers with respect to sea level, the value of BSL changes as follows [22].

$$BSL_n = \delta^m . BSL_s \quad \& \quad \delta = e^{(-A/8.15)} \quad (6)$$

Where BSL_n and BSL_s are the values of BSL in non-standard and standard conditions, respectively; A (km) is the height of the tower above sea level, and m is a constant that is obtained as follows. Here, S is the length of insulator string in meters, and CFOs is the standard value of CFO.

$$m = \frac{1.25CFO_s}{500S}\left(\frac{CFO_s}{500S} - 0.2\right) \quad (7)$$

In Fig. 3, the cumulative density distribution curve of CFO in non-standard conditions, CFOn, is shown for different values of height. As shown in this figure, with increasing height, the insulation strength of the insulator string decreases.

In this paper, the weighting parameter W is proposed to implement the level of vulnerability caused by the height above sea level.

$$W = 1/\delta^m \quad (8)$$

Where δ and m can be calculated from (1) and (2). The weighting coefficient W is first calculated using the height profile of the corresponding segment of the line; this coefficient modifies the overvoltage amplitude as the height increases. Therefore, in vulnerable points along the line, the overvoltages become more noticeable. In Table 2, the height profile of the line under study and the selected weighting function are shown for each candidate point.

Table 2. Transmission line profile and the proposed W for BSL=650 kV

Candidate Node	D_0	D_1	D_2	D_3	D_4	D_5
Distance From Station (km)	260	240	220	200	180	160
Number of towers	50	50	50	50	50	160
Altitude (m)	2200	2306	1730	1100	999	1104
W	1.017	1.018	1.014	1.009	1.008	1.009
Candidate Node	D_5	D_6	D_7	D_8	D_9	D_5
Distance From Station (km)	160	140	100	60	40	160
Number of towers	160	140	100	60	40	160
Altitude (m)	1104	1334	1505	900	800	1104
W	1.009	1.011	1.012	1.007	1.006	1.009

3. PRE-STRIKE VOLTAGE

From the theoretical point of view, the switching transient overvoltage during line energization will be zero if the CB is closed at the zero-crossing point of the instantaneous voltage. In practice, however, due to the reclosing time of the poles, the insulation strength of the breaker contacts and the imprecise operation of the controller, the optimal closing time does not match the zero-crossing point [23]. Therefore, for optimal operation of CBs, the uncertainties of the above mentioned cases should be modeled. In Fig. 4, it can be seen that before zero, because of a reduction in insulation strength over the distance between the contacts, a voltage is created before the closing instant, i.e., the pre-strike voltage. First, for simplicity, it is assumed that the line TC is zero in this case. In this paper, the presence of TC on the line side is generalized. In Fig. 4, t_c denotes the CB closing instant. Time t_d is a correction for the optimal closing instant, which is a function of allowable voltage, the number of ring chambers, closing speed of CB and system frequency, and it is defined as follows [20]:

$$t_d = \frac{U_m \sin(\omega . Dt)}{dU_s / dt} \quad (9)$$

where U_m is the maximum value of voltage, ω is the angular frequency and U_s is the insulation strength characteristic of the distance between the two contacts of the CB, which is assumed to be linear.

In the CS simulation, statistical modeling of imprecise operations of the CB and controller is performed in ATP using statistical switches. Accordingly, to implement this operation, tm, the mean value of the closing instant is associated with a standard deviation; tm can be obtained from the following equation:

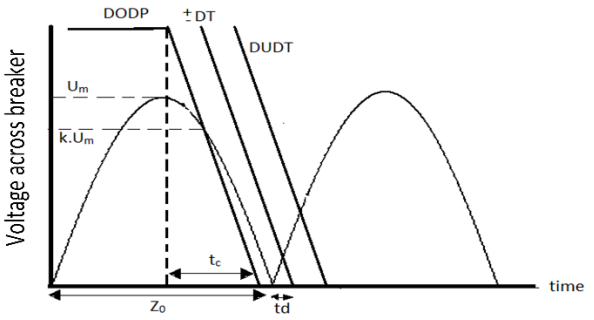

Fig. 4. Closing instant of CB [14]

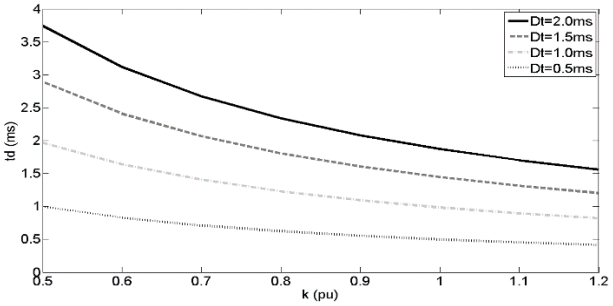

Fig. 5. Delay Curve for the prestrike voltage effect

$$t_m = t_0 + t_d - t_c \tag{10}$$

where t_c is calculated as follows:

$$t_c = \frac{DOP}{DUDT} \tag{11}$$

where DOP is the voltage strength characteristic of the CB in the open position, and DUDT is the slope of air gap voltage strength between contacts during the closing operation. The value of optimal closing instant delay varies with the allowable voltage. This delay depends on the closing speed of CB, and in this study, it is equal to the system frequency according to (4). The parameter D_t denotes the instant when the pre-arcing voltage occurs.

If the TC is assumed to be zero, then z_0 denotes the zero-crossing instant, and the delay curve is in accordance with Fig. 5. Therefore, in the event of the occurrence of pre-arcing voltage at a given instant, a smaller time delay is required for a higher peak of instantaneous voltage when the voltage across contacts becomes zero. In Fig. 5, for a given value of Dt, the suitable time delay is given in terms of k, from which the appropriate time delay (td) can be extracted.

To include the TC, in this paper, it is proposed that z0 is obtained from another simulation that simulates the controlled closing. Accordingly, the simulation strategy is proposed in the next section.

4. CS STRATEGY

The TACS-controlled switch (type 13) is used to implement the CS in ATP. This CB will be closed if a positive signal is applied to its controller. Therefore, to obtain the parameter z_0, it is necessary to replace "STAT" with TACS in the circuit of Fig. 2. In this situation, to prevent a multi-Frequency error, it is suggested that a DC trapped charge source is used.

The main problem is the effects of electromagnetic induction of improper closing instants, which are possible in the process of closing and lead tounreasonable overvoltages. Therefore, to solve this problem and to simulate the worst-case realization of overvoltages, it is suggested that the following relationships are met while the best closing instant is being searched.

$$V_{lA}(t) \le 1pu \tag{12}$$

$$V_{lB}(t) \le 1pu \tag{13}$$

$$V_{lC}(t) \le 1pu \tag{14}$$

where V_{lA}, V_{lB}, and V_{lC} are the line side voltages of the CB before closing phases A, B and C. Equations (7) to (9) guarantee that the TC voltage amplitude reaches 1 pu with opposite polarity.

In Ref. [24], the worst case of TC voltage with opposite polarity and an amplitude of 1 p.u. is identified. It is expected that if such conditions are provided for the CS strategy before the CB is closed, then the worst case of switching transients will be simulated. Therefore, the above equations have been presented for this purpose.

Searching for an appropriate time delay command requires trial and error in the simulation process. The proposed procedure for the command time delay is illustrated in Fig. 6.

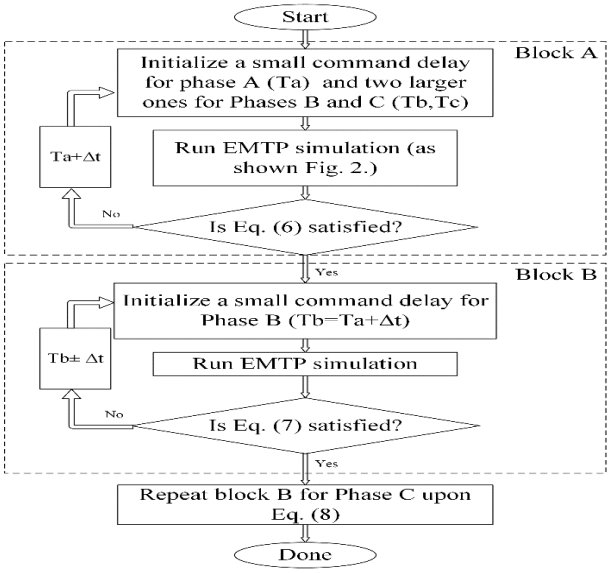

Fig. 6. Flowchart of the proposed method for CS

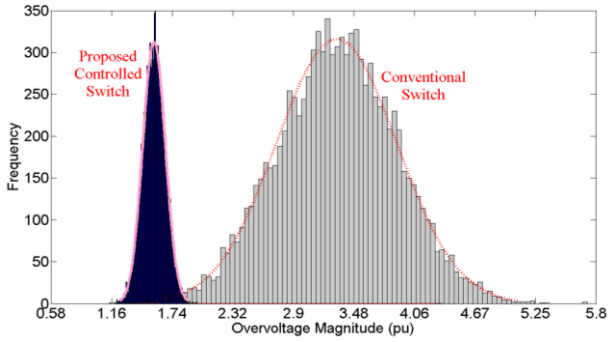

Fig. 7. Comparison of distributions of overvoltages of the proposed and conventional CS (V_{base}=342928 volts)

The randomly selected command delay for phase A is small, while much larger values are selected for phases B and C. Consequently, the effects of interaction among phases due to simultaneous closing are avoided. After executing the next step, when the command delay for phase A is found, the same process is executed for phases B and C, so that the time base for each phase is the closing time of the previous phase. Therefore, the time delays for phases A, B and C for the line SA913 are 14.38, 14.7 and 18.1 ms, respectively. In Fig. 7, the distributions of overvoltages of the proposed CS and conventional switching are shown for a line with a length of 400 km. In this case, the mean overvoltage of the proposed CS has been reduced by 52.69% compared to the conventional one.

Another fundamental problem that should be considered about the capabilities of the proposed method is its response to TC voltage fluctuations in the presence of a reactor at the end of the line.

4.1. Compensating reactor

In the past, parallel compensation was used to mitigate SOVs [25]. With the advent of zinc oxide surge arresters, this method of SOV mitigation was abandoned. However, parallel reactors are used in transmission lines to control steady-state voltage. The inductive nature of a reactor and the capacitive nature of a transmission line lead to a complex RLC circuit. Under the simulation of TC voltage, this circuit generates intense voltage fluctuations during the reclosing of the transmission line. The fluctuating voltage can be expressed as follows [10]:

$$V_{TL}(t) = V_{trp} - (V_{trp} - V_{TL0})\cos(\omega t) \quad (15)$$

where V_{trp} denote the TC, V_{TL0} is the initial fluctuating voltage. The frequency of voltage fluctuations is equal to the natural frequency of the RLC circuit as follows:

$$\omega = \frac{1}{\sqrt{LC}} \quad (16)$$

Here, L and C denote, respectively, the equivalent inductance and capacitance of the transmission line seen from the substation.

The basic issue is the inconvenience that the TC fluctuations cause for searching the best closing instant in CS. Accordingly, the simultaneous presence of a compensating reactor and TC has been avoided in most of the previous studies [26, 27]. The simultaneous presence of the compensating reactor and TC cause extreme fluctuations and impede the search for closing instant. In this paper, two strategies are proposed for executing the algorithm of Fig. 6 in the presence of the compensating reactor.

First strategy: to wait for closing after the TC fluctuations are suppressed, which is usually less than one second. Although this solution seems to be appropriate, the time for the suppression of the fluctuations depends on some factors, such as the linear wave impedance, the reactor capacity, the TC amplitude and the delay in closing instant.

Second strategy: This solution is more precise and more general than the previous strategy, and it is based on the fact that by reducing the time step (Δt) in the flowchart of Fig. 6, according to Eq. (10), the closing can be accomplished in the presence of fluctuations:

$$\Delta t \le \frac{1}{10\sqrt{LC}} \quad (17)$$

where L and C denote, respectively, the equivalent inductance and capacitance of the transmission line seen from the substation. As a rule of thumb, Δt is about 0.01 ms for the 400 kV line under study. Therefore, the optimal closing instants are 17.39, 17.67 and 18.17 ms.

The simulation results indicate that the installation of reactor has a minor effect on CS overvoltage, and reduces the amplitude of SOV by less than 8%. Therefore, although the implementation of the reactor for finding the best closing instant is challenging, it is not important to consider the reactor as the neural network input parameter for predicting SOVs.

5. ESTIMATING MAXIMUM OVERVOLTAGE

From the previous discussion, it can be concluded that the simulation of CS transients for calculating the maximum overvoltage is a complicated and time consuming process. Moreover, the addition of a new transmission line changes the SOV of other transmission lines of the substations at the beginning and the end of the line. Therefore, an operator needs to know the best sequence of energization of the lines of a substation. Calculating the overvoltages at the moment of lines

energization is not possible for the operator. To overcome this challenge, in this paper, an artificial neural network is proposed that can be replaced with the simulation of ATP transient, and can be used to estimate the maximum overvoltage in the operation stage or even in the design stage. To define the proposed network, the parameters that affect the maximum overvoltage of the line must be identified.

5.1. Factors affecting maximum overvoltage amplitude

These factors that depend on the network structure include line length and the impedance behind the source [28]. Of course, other parameters, such as the nature of the source, the presence of arresters, etc., affect the overvoltage amplitude of the conventional CBs, while they do not affect the overvoltage of closing instant control CBs [29].

Typically, with increasing length, the range of SOV distribution increases. Figure 8 shows the SOV distribution in terms of the change in line length.

As shown in Fig. 8, with increasing line length, the mean value of overvoltages increases, and the spread of the distribution changes. In some lengths, this pattern is reversed. The reason for this is the resonance between the capacitance and inductance of the line for the harmonic content of the switching waveform. Therefore, the effect of the line length is completely non-linear and irregular.

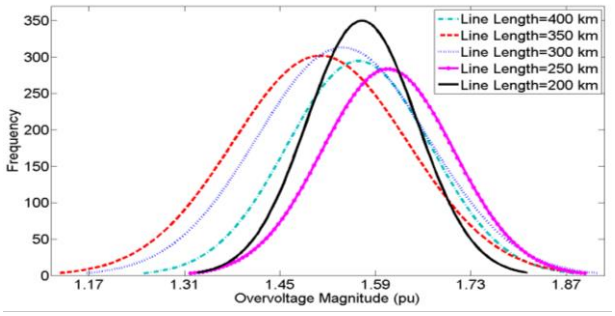

Fig. 8. Effect of increasing in line length on the CS overvoltage distribution (V_{base}=342928 volts)

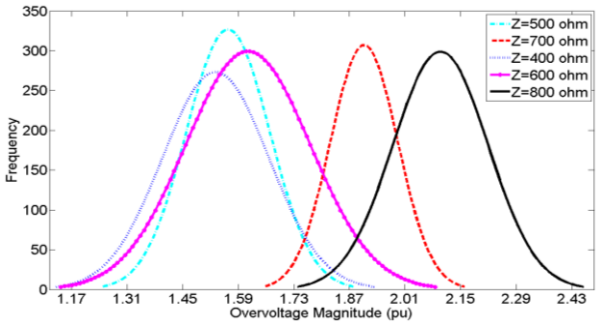

Fig. 9. Effect of impedance behind the source on the distribution of controlled SOV(V_{base}=342928 volts)

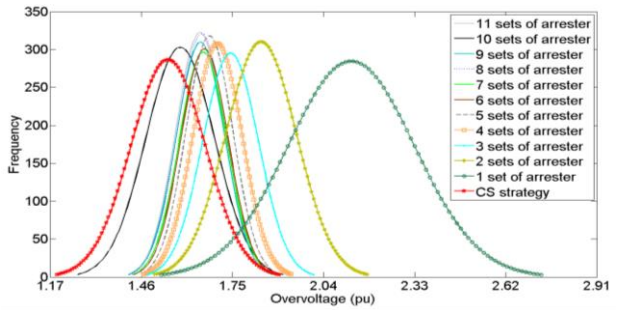

Fig. 10. Effect of installing arrester on the distribution of controlled SOV (V_{base}=342928 volts)

With the development of the power grid and the addition of new lines, the impedance behind the source of the existing lines changes, and thus, the maximum overvoltage amplitude in the line changes. The effect of installing surge arresters on the switching overvoltage distribution is shown in Fig. 10. The installed arresters are is ABB Exlim P, with rated voltage 330 kV and a maximum system voltage of 420 kV [30].

It is worth mentioning that the development of a power grid usually involves the addition of new transmission lines, and elongation (curtailment) of an existing line does not make sense. However, due to the high impact of changing the length, this parameter should be considered as the input parameter of the neural network.

Another effective parameter is the value of the Thevenin impedance of the feeder substation in the line (source power). Figure 9 shows the effect of this parameter. It is clear from Fig. 9 that for short-circuit levels less than the value of the surge impedance loading (SIL), the source impedance is insignificant. However, for short-circuit levels larger than SIL, the mean of the distribution increases with increasing source impedance.

In this figure, the effect of installing 11 sets of surge arresters (each set with three arresters) along the transmission line is shown. The arresters are installed at the candidate points shown in Fig. 2. The highest overvoltage occurs for one set of arresters installed at the end of the line (the rightmost distribution shown by green dotted line); and the lowest overvoltage occurs for installing arresters along the whole line (the distribution shown by solid black line). However, the distribution of CS has also less overvoltage values compared to all cases of arrester installation; that is, the CS overvoltage is not sufficiently large to stimulate the arrester to discharge. Therefore, it can be stated that the high effectiveness of the proposed CS mitigates SOV so that there is no need for involving surge arresters to mitigate the overvoltages.

5.2. Necessity of defining RBFN

ATP simulation is only considered to obtain the statistical distribution of overvoltages [22]. The transmission line insulation level and the height profile can be applied to ATP outputs, so SOVs can be calculated. The implementation of the network needs information on power system transients and ATP simulation. ATP, which is based on EMTP cards with FORTRAN machine language, is not a user-friendly environment. Statistical switching is time-consuming and requires many iterations. Thus, the whole process is complex, time-consuming and inconvenient. The complexity causes serious human errors in the stage of insulation coordination designing. Moreover, during system operation, some transmission lines may be indented to be re-energized after a partial outage. In the operation stage, the operator should determine the switching sequence, which is safe and may lead to minor outcomes, so ATP cannot be investigated in the operation stage.

In this paper, instead of ATP simulations, the proposed RBFN is used. The meta-model makes it possible for the designers to choose the insulation level by considering the height profile easily without making any mistake. Additionally, this model is useful for the operators to choose proper sequence of switching transmission lines that are fed by CS.

5.3. Radial neural network

Radial neural network or RBFN is one of the most widely used powerful tools with a simple structure for predicting the output of complex systems using sample input/output data [31]. These networks are also used for modelling and controlling nonlinear systems. The widespread use of these networks is due to the simplicity of their structure compared to other neural networks, i.e., complex multilayer perceptrons. Radial basis function (RBF) networks include a hidden layer connected to the network output. In an RBF network, training is essentially related to the search for multi-dimensional levels, so by using training information, the output is well estimated [32]. The main architecture of BRFN consists of a three-layer network as shown in Fig. 11.

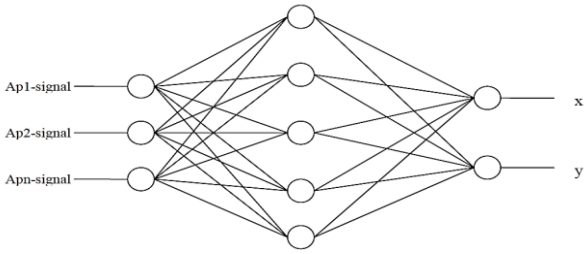

Fig. 11. Main architecture of BRFN

The input layer only receives inputs with no processing. The second or hidden layer establishes a nonlinear adaptation between the input space and a space with usually larger dimensions; this layer plays an important role in transforming nonlinear patterns into linearly separable patterns. Finally, the third layer produces a weighted sum along with a linear output. Such an output is useful if RBFN is used to approximate a function, but if the classification of the patterns is required, then a hard-limiter or a sigmoid function can be used for the output nerves to generate zero or one output values.

As explained, the distinctive feature of this network is the processing in the hidden layer. The hidden layer function can be written as follows [32]:

$$F(x)=\sum_{j=1}^{p} w_j \phi(\|x-u_j\|) \tag{18}$$

This equation shows that for approximating F, function p is used, which is a radial function with u_j denoting the gravity centers. The symbol ‖ denotes the distance function in the R_n space, which is usually the Euclidean distance. Because the curve of the radial circuit functions is symmetrical, the hidden layer neurons are known as radial function neurons.

To generate RBF data of the network under study, 20 possible lengths and 20 impedance values behind the source are defined. The results show that the mentioned number of input group data (20 pairs for each input) is sufficient. By using statistical switching simulation, the maximum overvoltage is also specified. The weights resulting from changes in the height profile will be applied by the RBFN after predicting the maximum overvoltage. The method proposed for estimating the SOVs of CS is shown in Fig. 12; i.e., the whole procedure of modelling, controlling, training and estimating the SOV in CS.

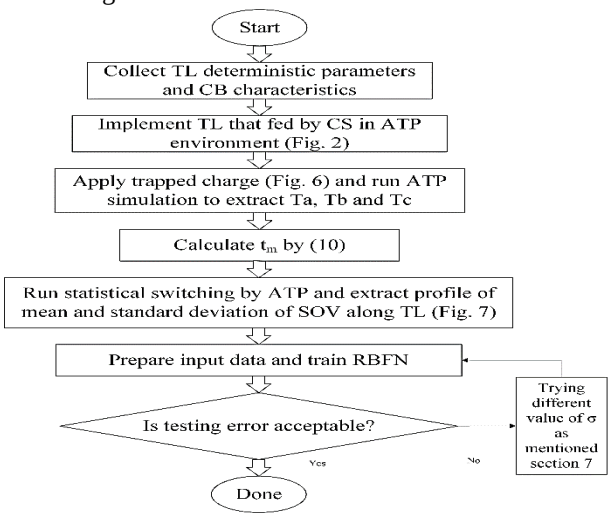

Fig. 12. The proposed flowchart to replicate the paper results

Table 3. Results of the proposed RBFN and ATP simulation

Name	End Station	Length (km)	Source Power (MVA)	Max. of SOV in kV		Error (%)
				EMTP	RBFN	
SA912	Khoram abad	225	18331.2	620.65	608.86	1.9%
	Karkhe	225	3513.35	544.5	545.04	0.1%
SA913	Khoram abad	270	6961.46	550.89	565.76	2.7%
	Shomal Kuzestan	270	3579.26	609.8	529.84	3.2%
SL102	Kermansha	375	5091.29	600.35	602.15	0.3%
	Khoram abad	375	815.71	689.54	669.54	2.9%

The flowchart in Fig. 12 is used to replicate the paper results. As a result, the input-output data sets are obtained by deterministic data from the network. The intervals of line length and back impedance are introduced in Figs. 8 and 9. The strategy of Fig. 6 is applied to the case study of Fig. 2, and T_a, T_b and T_c are then obtained. Next, the closing time distribution is calculated by using Eqns. (9) – (11), and the test system is simulated statistically in 100 switching operations. The output of ATP is ten distribution functions of obtained overvoltages and maximum SOVs for each transmission line configuration.

6. SIMULATION RESULTS

Left To implement RBFN, the MATLAB software toolbox has been used. In order to properly train RBFN with the smallest training error, the input/output data is normalized. The data is then displaced and normalized in a way that the mean of data cluster becomes zero and the variance becomes one. Sixty percent of the entire dataset is intended for training, 20% for controlling the training process and 20% for random testing. The goal is to obtain zero error, and the optimal value of σ is chosen to be 0.4. The training error is low and equal to 1.3%. In Table 3, the overvoltage values are estimated by the RBF network and ATP simulation results are presented. Accordingly, the RBF network can well be used as an alternative to the SOV estimation in the process of lines energization by using CS. As expected, the lines energization from the point where the short-circuit power of the source is higher imposes lower overvoltage on the line insulators. Moreover, in the case of future network development, the above artificial network can easily search the resultant overvoltages and vulnerable points.

In Fig. 13, the weighted maximum overvoltage profile of the transmission line under study is shown. This line has been energized by the substation in the north of Khuzestan, and the produced overvoltage is low. As seen in this figure, without considering the effect of insulation strength weakening caused by the height profile, the end of the line experiences the highest overvoltage amplitude of 550 kV. After applying the weights associated with the strength weakening, the maximum overvoltage amplitude is 560 kV. In Fig. 14, the transient SOV at the end of the line (D_0, according to Fig. 2) is shown. The maximum SOV is equal to 550 kV.

The transient voltage across all phase is plotted in Fig. 14 with the optimal delay time of 18.1 msec (≈300000/[400000√2/√3]×[1/50Hz]). A TC voltage of 300000 V is selected for a 400 kV voltage level [24]. The terminals of phase C are closed once the voltages of the line and source become equal, which results in a small SOV value. A similar process is used for the other phases with a 120-degree difference based on their waveforms. The maximum SOV is equal to 435 kV. From Figs. 14 and 15, the value of TC is constant and equal to 1 p.u. (=342928 volts) before the CB is closed. The amplitude of maximum SOV is larger than the amplitudes of the SOVs of the three phases.

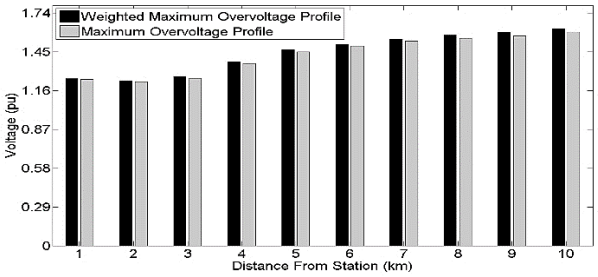

Fig. 13. Weighted maximum overvoltage profile of the line under study (V_{base}=342928 volts)

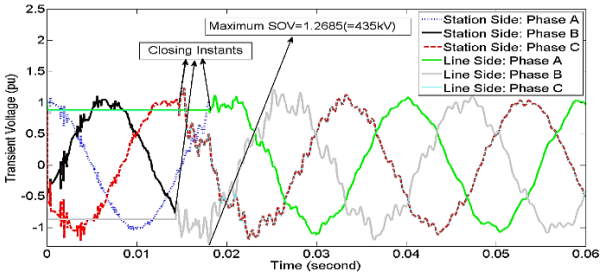

Fig. 14. Transient overvoltage across the CB

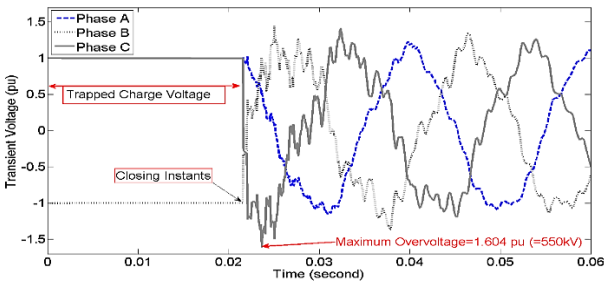

Fig. 15. Transient overvoltage at the end of line SA913 (V_{base}=342928 volts)

Table 4. Comparison between the proposed method and the method in [29]

	Risk criterion of Ref. [29]	The criterion of the proposed weight function of overvoltage
Without considering the height profile	0.0202	550.89
With considering height profile	0.022	560.47
Distance between the predicted vulnerable point and station (km)	260	260

However, in this case, no significant changes can be seen in the weighted overvoltage amplitude, while in high-altitude areas, the maximum overvoltage location may be changed and severe stress may be imposed on the network.

7. COMPARING RESULTS WITH PREVIOUS STUDIES

To confirm the method presented in this paper, a comparison has been made with the criteria used in the most recent reliable studies. In Ref. [29], a fuzzy-neural method is used to estimate the insulation risk of the transmission line. This reference uses the CS strategy for controlling overvoltages. The criterion used for transmission line insulation coordination is the insulation risk. Although this criterion is accurate, it suffers from some complexities. Consequently, to reduce the training errors, this reference has to use data screening techniques. This preparation of training data increases the computational burden. The other limitation of the utilized fuzzy-neural method is that it is single-output. Therefore, at least 10 fuzzy-neural networks must be trained for each line. In Table 4, the results of this paper are compared with the results of the strategy in Ref. [29]; a BSL of 650 kV has been considered for line SA913.

The height profile is not considered in the first row, while it is considered in the second row. By comparing these two cases, the capability of the proposed weighted overvoltage criterion can be evaluated. The third row measures the ability of the proposed method to predict the point vulnerable to switching overvoltage in the line. This point on the transmission line is important for the operator and insulation designer of the line.

As shown in Table 4, the height profile increases the risk of insulation failure by ([0.022-0.0202]/0.0202=) 8.9%; the corresponding weighted switching overvoltage increases by about 10 kV. In addition, the proposed indicators of both weighted risk and overvoltage exhibit the highest values at a distance of 260 km from the feeding substation. As can be seen from the results, the proposed method can correctly identify the high stress location and is consistent with the results of the previous study. The advantage of the proposed method is its simplicity and high precision of prediction. The calculation of risk is time-consuming and complicated; however, in addition to its simplicity, the proposed weighting method can be implemented quickly, and in the operation stage, this simplicity will be very helpful to the operator. Therefore, when the energization of multiple transmission lines is intended, the operator can choose the switching sequence based on the effective parameters to minimize the SOVs. In addition, the proposed RBFN can be used to determine which end of the transmission line should be energized to have the minimum switching overvoltage. This is because the power of feeding substation is different at each end of the line, so the amplitude of the SOV is also different at each end.

8. CONCLUSION

In this paper, an RBF network was trained to estimate the maximum SOV of the line fed by CS. For this purpose, a sensitivity analysis was presented to consider all the parameters affecting the overvoltage amplitude. The considered parameters included line length, impedance behind the source, TC and pre-strike voltage. Based on the proposed control strategy, the mean of overvoltage distribution is reduced by 53% compared to the case with conventional CBs. To generalize the application of the proposed strategy, a method was developed to use the proposed strategy in the presence of fluctuations resulted from including a reactor.

Due to the complexity of ATP simulation, and the necessity for replacing the ATP simulation with the RBF network, the training data was provided using simulations. The results of the paper confirmed the high accuracy of prediction with an error of less than 3%. Because the insulation strength weakens as the altitude of the line increases with respect to sea level, a new weighting factor was proposed to correct the maximum overvoltage amplitude of the line. Finally, to verify the results, the proposed strategy was compared with previous studies.

Acknowledgments

The authors of this paper would like to gratefully thank Mohsen Akafi Mobarakeh and Dr. Reza Shariatinasab for their valuable suggestions and guidance.

REFERENCES

[1] R. Shariatinasab, J. Safar and H. Falaghi, “Optimisation of arrester location in risk assessment in distribution network”, *IET Gener. Transm. Distrib.*, vol. 8, pp. 151-

159, 2014.
[2] M. Akafi, "Estimation of SOV on transmission lines using fuzzy method", M.S. thesis in Electrical Engineering, Power Systems, Faculty of Engineering The University of Birjand., Iran, 2012.
[3] N. Eskandari and S. Jalilzadeh, "Electrical load manageability factor analyses by artificial neural network training", *J. Oper. Autom. Power Eng*., vol. 7, pp. 187-195, 2019.
[4] A. Deihimi and A. Rahmani, "An intelligent method based on WNN for estimating voltage harmonic waveforms of non-monitored sensitive loads in distribution network", *J. Oper. Autom. Power Eng.*, vol. 6, pp. 13-22, 2018.
[5] D. Thukaram, H. Khincha and S. Khandelwal, "Estimation of switching transient peak overvoltages during transmission line energization using artificial neural network", *Electr. Power Syst. Res.*, vol. 76, 2006.
[6] S. Taher and I. Sadeghkhani, "Estimation of magnitude and time duration of temporary overvoltages using ANN in transmission lines during power system restoration", *Simul. Modell. Pract. Theory*, vol. 18, 2010.
[7] R. Shariatinasab et al., "Optimization of surge arrester's location on EHV and UHV power networks using simulation optimization method", *IEEJ Trans.*, vol. 128, 2008.
[8] R. Shariatinasab, M. Akafi and M. Farshad, "Estimation of SOV on transmission lines using neuro-fuzzy method", *Intell. Syst. Electr. Eng.*, vol. 3, pp. 55-66, 2013.
[9] A. Hamza, S. Ghania, A. Emam and A. Shafy, "Statistical analysis of SOV and insulation coordination for a 500 kv transmission line", *19th Int. Symp. High Voltage Eng*., pp. 1-4, 2016.
[10] H. Seyedi and S. Tanhaeidilmaghani, "New CS approach for limitation of transmission line SOV", *IET Gener. Transm. Distrib.*, vol. 7, 2013.
[11] M. Atefi and M. Sanaye-Pasand, "Improving controlled closing to reduce transients in HV transmission lines and circuit breakers", *IEEE Trans. Power Delivery*, vol. 2, 2013.
[12] M. Sanaye-Pasand, , M. Dadashzadeh and M. Khodayar, "Limitation of transmission line SOV using switchsync relays", *Int. Conf. Power Syst. Transients*, pp. 1-6, 2005.
[13] D. Lin et al., "An adaptive reclosure scheme for parallel transmission lines with shunt reactors", *IEEE Trans. Power Delivery*, vol. 30, pp. 2581-89, 2015.
[14] P. Mestas, M. Tavares and A. Gole, "Implementation and performance evaluation of a reclosing method for shunt reactor-compensated transmission lines", *IEEE Trans. Power Delivery*, vol. 26, pp. 954-962, 2011.
[15] K. Dantas, W. Neves and D. Fernandes, "An approach for controlled reclosing of shunt-compensated transmission lines", *IEEE Trans. Power Delivery*, vol. 29, pp. 1203-11, 2014.
[16] K. Bhatt, B. Bhalja and U. Parikh, "Controlled switching technique for minimization of switching surge during energization of uncompensated and shunt compensated transmission lines for circuit breakers having pre-insertion resistors", *Int. J. Electr. Power Energy Syst.*, vol. 103, pp. 347-359, 2018.
[17] I. Ibrahim and H. Dommel, "A knowledge base for switching surge transients", *Int. Conf. Power Syst. Transients*, pp. 1-6, 2005.
[18] M. Cervantes et al, "Simulation of SOV and validation with field tests", *IEEE Trans. Power Delivery*, vol. 33, 2018.
[19] J. Das, "Transients in electrical systems: analysis, recognition, and mitigation", the McGraw-Hill Companies, USA, 2010.
[20] R. Rocha and J. Tavora, "EMTP model for CS simulation by means of TACS routine", *Int. Conf. Power Syst. Transients*, pp. 254-259, 1997.
[21] A. Hileman, "Insulation coordination for power systems", Marcel Dekker Inc., New York, 1999.
[22] R. Shariatinasab et al., "Probabilistic evaluation of optimal location of surge arrester on EHV and UHV networks due to switching and lightning surges", *IEEE Trans. Power Delivery*, vol. 24, 2009.
[23] R. Smeets et al., "Switching in electrical transmission and distribution systems", John Wiley & Sons, 2014.
[24] S. Hosseinian, M. Abedi and B. Vahidi, "Digital computer studies of random switching of Iranian standard 400 kV lines", *3rd Int. Conf. Properties Appl. Dielectric Mater.*, pp. 542–545, 1991.
[25] A. Clerici, G. Ruckstuhl and A. Vian, "Influence of shunt reactors on switching surges", *IEEE Trans. Power Apparatus Syst.*, vol. 89, 1970.
[26] W. Hofbauer et al., "Controlled closing on shunt reactor compensated transmission lines - Part II", *IEEE Trans. Power Delivery*, vol. 12, 1997.
[27] K. Dantas, W. Neves and D. Fernandes, "An Approach for controlled reclosing of shunt-compensated transmission lines", *IEEE Trans. on Power Delivery*, vol. 29, 2014.
[28] Cigre Working Group, "SOV in EHV and UHV systems with special reference to closing and reclosing transmission lines", *Electra 30*, pp. 70-122, 1973.
[29] M. Hasanpour, M. Ghanbari and V. Parvin-Darabad, "Estimation of switching surge flashover rate of point on wave switching over-voltages along transmission line by adaptive neuro-fuzzy inference system meta-model", *IET Sci. Meas. Technol*, vol. 13, pp. 1326-1334, 2019.
[30] ABB, "Controlled switching, buyer's & application guide", (ABB, Ludvika, Sweden, 4th edn.), pp. 33-54, 2013.
[31] A. Alexandridis et al, "A fast and efficient method for training categorical radial basis function networks", *IEEE Trans. Neural Network Learn. Syst.*, vol. 28, 2017.
[32] A. Alexandridis, E. Chondrodima and H. Sarimveis, "Radial basis function network training using a nonsymmetric partition of the input space and particle swarm optimization", *IEEE Trans. Neural Network Learn. Syst.*, vol. 24, pp. 219-230, 2013.